A paradigm for modeling and computation of gas dynamics

Kun Xu[1,a)] and Chang Liu[2,b)]
[1]*Department of Mathematics, Department of Mechanical and Aerospace Engineering, Hong Kong University of Science and Technology, Peninsula, Hong Kong*
[2]*Department of Mathematics, Hong Kong University of Science and Technology, Peninsula, Hong Kong*

(Received 1 August 2016; accepted 9 January 2017; published online 2 February 2017)

In the continuum flow regime, the Navier-Stokes (NS) equations are usually used for the description of gas dynamics. On the other hand, the Boltzmann equation is applied for the rarefied flow. These two equations are based on distinguishable modeling scales for flow physics. Fortunately, due to the scale separation, i.e., the hydrodynamic and kinetic ones, both the Navier-Stokes equations and the Boltzmann equation are applicable in their respective domains. However, in real science and engineering applications, they may not have such a distinctive scale separation. For example, around a hypersonic flying vehicle, the flow physics at different regions may correspond to different regimes, where the local Knudsen number can be changed significantly in several orders of magnitude. With a variation of flow physics, theoretically a continuous governing equation from the kinetic Boltzmann modeling to the hydrodynamic Navier-Stokes dynamics should be used for its efficient description. However, due to the difficulties of a direct modeling of flow physics in the scale between the kinetic and hydrodynamic ones, there is basically no reliable theory or valid governing equations to cover the whole transition regime, except resolving flow physics always down to the mean free path scale, such as the direct Boltzmann solver and the Direct Simulation Monte Carlo (DSMC) method. In fact, it is an unresolved problem about the exact scale for the validity of the NS equations, especially in the small Reynolds number cases. The computational fluid dynamics (CFD) is usually based on the numerical solution of partial differential equations (PDEs), and it targets on the recovering of the exact solution of the PDEs as mesh size and time step converging to zero. This methodology can be hardly applied to solve the multiple scale problem efficiently because there is no such a complete PDE for flow physics through a continuous variation of scales. For the non-equilibrium flow study, the direct modeling methods, such as DSMC, particle in cell, and smooth particle hydrodynamics, play a dominant role to incorporate the flow physics into the algorithm construction directly. It is fully legitimate to combine the modeling and computation together without going through the process of constructing PDEs. In other words, the CFD research is not only to obtain the numerical solution of governing equations but to model flow dynamics as well. This methodology leads to the unified gas-kinetic scheme (UGKS) for flow simulation in all flow regimes. Based on UGKS, the boundary for the validation of the Navier-Stokes equations can be quantitatively evaluated. The combination of modeling and computation provides a paradigm for the description of multiscale transport process. *Published by AIP Publishing.* [http://dx.doi.org/10.1063/1.4974873]

I. INTRODUCTION

The theoretical study of gas dynamics is mostly based on the analytical and numerical solutions of the Euler and Navier-Stokes equations. The modeling of the NS is obtained from the conservative physical laws, the inclusion of constitutive relationships for the stress and strain, and the relationship between the heat flux and temperature gradient. But, the scale for the validity of the NS equations has never been clearly defined, even though it always refers to the hydrodynamic one. The boundary for the valid application of NS equations is unclear, especially for the hypersonic flow study. For a hypersonic flow around a flying vehicle, different flow physics may emerge at different regions, such as the highly non-equilibrium shock layer, low density trailing edge, and the wake turbulence. Fig. 1 presents the local Knudsen number around a flying vehicle at Mach number 4 and Reynolds number 59 373. As shown in this figure, the local Knudsen number can cover a wide range of values with five order of magnitude difference. It seems that a single scale governing equation can be hardly applicable in an efficient way to recover flow physics in all regimes. On the other hand, the Boltzmann equation is derived on a well-defined modeling scale, which is the particle mean free path and the particle mean traveling time between collisions.[4] This is also the finest physical resolution of the Boltzmann equation. Only under such a modeling scale, the particle transport and collision can be separately formulated. In the kinetic scale, the particle distribution is modeled as a field, and the Boltzmann equation becomes a statistical modeling equation. The Boltzmann equation can be numerically

[a)]Email: makxu@ust.hk
[b)]Email: cliuaa@connect.ust.hk

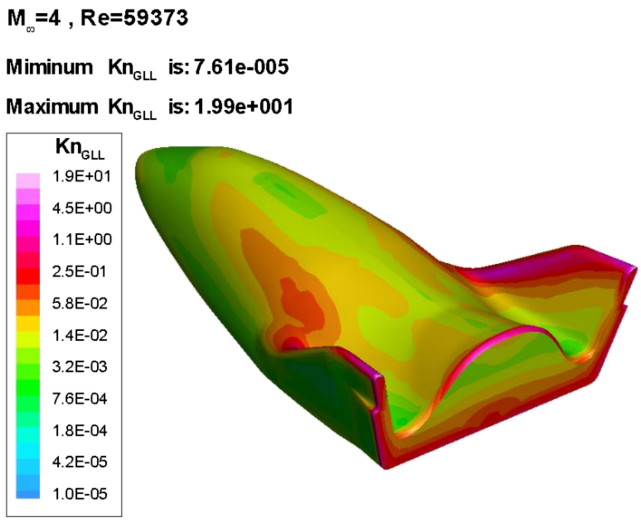

FIG. 1. Local Knudsen number around a flying vehicle at Mach number 4 and Reynolds number 59 373 calculated by Jiang using a unified gas kinetic scheme.[7]

solved through the Direct Simulation Monte Carlo (DSMC) method[3] or the direct Boltzmann solver[1] with the numerical cell resolution on the same scale. For example, for DSMC the cell size is usually smaller than the particle mean free path. Therefore, it becomes difficult to solve multiple scale problem with a required cell resolution always on the particle mean free path. Since the Boltzmann equation has a much refined resolution in comparison with hydrodynamic one, in order to derive the NS equations, a coarse-graining process has to be used. One of the most successful theoretical studies of the Boltzmann equation is the Chapman-Enskog expansion, where with a proper stretching of the space and time scales, the NS equations can be obtained. It is fortunate that due to the separation of scales between NS and Boltzmann equations, both equations can be confidently used in their respective scales. Even though the NS equations can be correctly derived form the Boltzmann equation, there are tremendous difficulties to derive other equations between the kinetic and hydrodynamic scales, which span over the whole non-equilibrium flow regime. The difficulties are associated with the following reasons. First, how to define a continuously variational modeling scale between the kinetic and hydrodynamic ones to derive the equations. Second, what kind of flow variables can be used to describe the flow motion between these two limits. Third, in the transition region there is no clear scale separation and the conventional mathematical tool may not be applicable. For the NS equations, there are only five flow variables, such as mass, momentum, and energy, to describe the dynamics.[8] However, for the Boltzmann equation, there are theoretically an infinite number of degrees of freedom due to the capturing of individual particle movement. How many flow variables should be properly used between these two limiting cases to recover all possible non-equilibrium states are basically unclear. All extended thermodynamic theories or irreversible thermodynamics are focusing on the study of flow close to equilibrium only. In fact, we have no much knowledge about the non-equilibrium physics between the hydrodynamic and kinetic scales.

In reality, for the gas dynamics, the use of distinct governing equations, such as NS and Boltzmann, is limited to describe the flow physics in their corresponding scales and these descriptions are incomplete. With the variation of the modeling scale, there should exist a continuous spectrum of dynamics between these two limits. The multiple scale equation is needed to capture the scale-dependent flow physics from the kinetic to the hydrodynamic ones. With great difficulty by choosing an appropriate modeling scale in the theoretical study, the computation provides us an opportunity to do direct modeling with a freely varying scale, which is the mesh size and time step. In other words, the traditional procedure to derive the governing equation can be extended to a discretized space to construct the corresponding governing equations as well. Therefore, the numerical algorithm itself can be considered as a process of constructing governing equation and obtaining its evolution solution. Based on the direct modeling on the mesh size and time step, a unified gas-kinetic scheme (UGKS) has been developed for the flow description in all regimes.[15,17] The main purpose of this paper is to point out the way beyond the traditional numerical PDE methodology for the gas dynamic study. At the same time, we are going to use the direct modeling scheme to validate the NS equations through case studies. The UGKS is based on a direct modeling of physical law in a control volume with limited cell resolution, which is distinguishable from direct discretization of the well-defined kinetic equation. Here in UGKS, the cell size and time step play dynamic roles in representing the flow physics. The paradigm for modeling and computation is useful in the study of other multiple scale transport process, such as radiative transfer and plasma simulation.[10,13]

II. GAS DYNAMICS MODELING

Now consider a box with a length scale L, such as with a value $L = 0.01$ m, and the box is supposed to hold a certain amount of molecules, see Fig. 2. Under the standard atmospherical condition, the number density of molecules is $n = 2.687 \times 10^{25}$ m^{-3}. In the following mental experiment, we assume that the number density of the particles inside the box can be changed significantly to different levels. And we define the diameter of the molecule as d, which is on the order of $d = 3.7 \times 10^{-10}$ m, and the mean free path between the collisions of molecules ℓ. The relationship between d and ℓ is $\ell = 1/\sqrt{2}(\pi n d^2)$, such as 6.1×10^{-8} m in the standard atmospheric condition. The density of the gas inside the box can be defined as $\rho = nm$ and m is the molecular mass. The Kundsen number defined as $\mathrm{Kn} = \ell/L$ indicates the rarefaction of the

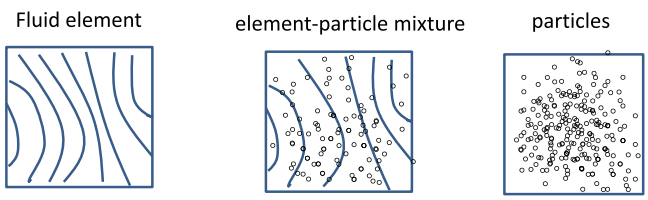

FIG. 2. Modeling gas dynamics from the fluid element in hydrodynamic scale (left) to the particle representation in kinetic scale (right) through the non-equilibrium regime with a variable degrees of freedom (middle).

molecular distribution. The scales from the molecular diameter to the dimension of the box can be varied across a scale of ten orders of magnitude. The box can be considered as a modeling scale.

Let us assume a constant gas temperature T and different particle number density inside the box. In the kinetic limit, such as at the Knudsen number $Kn \simeq 1$, the molecules can freely move through the box from one end to the other side, and the interactions between the molecules and the walls are equally important, where the particle free transport can be used to model the flux on the wall. As the Knudsen number reduces with the increment of molecules inside the box, such as $Kn = 0.1$, each particle may take hundreds of collisions to move from one end to the other end of the box. At the same time, each particle can still move freely to anywhere inside the box. There is full penetration among all molecules. With the Boltzmann modeling, the flow physics under such a condition can be easily solved using a mesh size on the order of the particle mean free path. In the Boltzmann solver, particle free transport and collision can be treated separately as the mesh size is smaller than the particle mean free path. But, if the mesh size gets to the size of the box, the free transport mechanism cannot be used to model the flux on the wall anymore. If there is no bulk velocity for the molecules inside the box, for a system with $0.1 < Kn < 10$, information inside the box can propagate from one end to another end through molecular motion with a speed $C_r \sim \sqrt{RT}$, where $R = k/m$ is the gas constant and k is the Boltzmann constant, as shown in the right sub-figure in Fig. 2.

Before we consider the system with a continuous reduction of Knudsen number, let us go to another limit, i.e., the hydrodynamic one. Under such a situation, such as at the standard atmospheric condition, there is an order of 10^{19} particles inside the box. At such a limit, the Knudsen number can reach an extremely small value, as low as 10^{-6}. If we still use the Boltzmann modeling to study the system, we need a high resolution calculation with the mesh size on the order of 10^{-8} m. For such a system, due to the high molecular density and small particle mean free path, in order to study the system efficiently, the fluid element modeling is used and the traditional hydrodynamic equations are accurate enough for the description of flow structure in such a large scale relative to particle mean free path. Here we need to use a cell size on the thousands of mean free path, such as $\Delta x = 10^{-4}$ m. With the intensive particle collisions in the scales 10^{-8} m and 10^{-10} s, the exchange of the momentum and energy will equalize the temperature and macroscopic velocity locally. Therefore, the local equilibrium assumption can be achieved in the hydrodynamic scale 10^{-4} m. With the separation of the scales in the hydrodynamic and kinetic ones, the NS scale modeling for such a system can use the fluid element concept, where the molecules inside the box can be separated into different distinguishable elements with a gigantic amount of molecules inside each unit. Between the elements, there is pressure, viscous friction, and heat exchange, but there is no mass or molecules penetration due to individual isolated element approximation, such as the absence of mass diffusion term. The interactions between fluid elements are basically through waves, such as the left sub-figure in Fig. 2. This is also the foundation for using the equation of state of classical thermodynamics to each isolated fluid element. In other words, in the continuum NS limit, the intensive particle collision prevents the particle from free penetration between elements. The energy exchange, such as the work done by the force and the heat transfer, takes place through the boundary, such as the heat diffusion in the Fourier's law. In such a case, any information in the gas system will propagate through wave behavior, i.e., a process for each fluid element to push the neighboring one. This wave propagating process has the same speed as the molecular motion $C_c \sim \sqrt{RT}$ in the continuum limit. Only under the fluid element picture, there is a Lagrangian description for the gas dynamics, where the neighboring elements are always stuck together. Theoretically, the continuum gas dynamic equations are almost identical to the equations of elasticity. There is a lack of changing neighboring effect, which may have disadvantages in modeling and capturing specific flow behaviors, such as the flow separation, where different fluid elements from different places get together. The fluid element picture sometimes is associated with difficulties to cope with other requirements, such as the non-slip boundary condition. Under such a condition, a fluid element needs to be stretched forever in the boundary layer, which cannot be true. More importantly, for the NS equations there is no clear definition of the scale for the validity of the equation itself, such as the scale of element where the constitutive relationship can be faithfully applied. As analyzed by Sone,[12] the flow dynamics induced by temperature fields in the continuum limit is closely related to the flow behavior in the rarefied regime. The Navier-Stokes equations, which are supposed to describe the flow motion in the limit of vanishing mean free path, contain the mean free path effect through the dissipative coefficients. In other words, the NS equations give an incompleteness description of gas dynamics in the continuum limit, where ghost effect appears in the continuum limit. The molecular gas dynamics or kinetic theory gives a more truthful description. So, to figure out the validity regime for the NS equations is important in the current fluid dynamics research, especially in the study of hypersonic non-equilibrium flow, even in the so-called continuum regime.

Starting from the continuum limit, if the gas density inside the box is reduced, the length scale of the particle mean free path will increase. The assumption of the isolated fluid element will break down as the particle penetration effect emerges. With the further reduction of the gas density, the fluid element assumption has to be abandoned due to the intensive particle exchange among the neighboring fluid elements. During this process, both the pressure interaction (waves through fluid element) and particle penetration (particles free transport) will take effect, such as the middle figure in Fig. 2. In this regime, the information can propagate through the wave interaction and particle transport, which have the same speed of $C_m \sim \sqrt{RT}$. In terms of physical modeling, in such a scale, it is difficult to give a complete description of the flow system using fluid element picture or individual particle motion representation alone. Unfortunately, all extended hydrodynamic equations or moment equations derived from the Boltzmann equation are intrinsically based on the fluid element assumption, where only macroscopic flow variables are used in the governing equations. Besides different flow

variables used in different scales, to reach a macroscopic level of description, starting from the microscopic reality, a coarse graining process has to be used with changeable degrees of freedom. During this process, a certain amount of information gets lost and a corresponding uncertainty is added to the macroscopic description, such as the supplement of equation of state and the constitutive relationship from the fluid element approximation.

With the reduction of gas density, the degrees of freedom for an accurate description of the flow system increase continuously from the hydrodynamic to the kinetic level. In other words, the construction of the extended hydrodynamic equations with a fixed number of flow variables, such as Burnett, Super-Burnett, or moment equations, cannot give a complete representation. On the other hand, with a kinetic scale resolution everywhere, the direct use of the Boltzmann equation will be very expensive with a cell resolution on the mean free path scale all the times. The modeling scale for the Boltzmann equation is only on the particle mean free path and particle traveling time between collisions. This can be understood from its formulation. The left hand side of the Boltzmann equation is the particle free transport, which can be valid only in a scale with less than one particle collision. At the same time, the collision term on the right hand side is for the un-correlated colliding particles (molecular chaos), which cannot be true in time scale with multiple encounters for an individual particle. In fact, in the regime between the hydrodynamic and kinetic ones, for an efficient modeling, we need to consider the effect in a time and spatial scale with multiple collisions for an individual particle. The efficient modeling in a large scale in comparison with the particle mean free path is not a simple accumulating evolution solution of the Boltzmann equation with the resolution always in the mean free path scale. Instead, it is a direct modeling equation in a different scale, such as figuring out the governing equations directly in a scale with a resolution of 10 mean free path and 10 particle collision time. Unfortunately, there is no such a governing equation with variable degrees of freedom for the capturing of non-equilibrium effect in the transition regime. Furthermore, no proper flow variables have ever been defined to give a valid description for such a system, such as the mathematical description in a time scale with multiple particle collisions or in a spatial resolution with tens or hundreds particle mean free path. Therefore, this regime is basically unexplored even though we have two successful limiting governing equations, i.e., NS and Boltzmann, in two distinct and separate modeling scales. The inseparable or continuous variation of scales in the transition regime makes theoretical modeling difficult. The separation of particle free transport and collision in the Boltzmann modeling cannot be used in the scale with multiple particle collisions for individual particle. Even though it is difficult to construct a PDE-type formulation for such a variational scale, in fact we can directly get the discretized governing equations through the direct modeling of the gas evolution in the mesh size scale Δx, where $\ell/\Delta x$ is a fully free parameter. As shown in the numerical experiments, the physical solutions will be presented in a cell resolution with one-tenth to hundreds of particle mean free path. This requires the direct modeling to capture the flow physics in different scales.

In order to give a full description of gas dynamics at different scales, we have to construct valid governing equations for a continuous variation of flow physics. The parameter used in the modeling can be defined as the ratio of the mean free path over the cell size, the so-called cell Knudsen number $Kn_x = \ell/\Delta x$. Based on the direct modeling on the mesh size scale, a continuous description of flow physics has been obtained in the unified gas-kinetic scheme (UGKS),[15,17] which covers the NS and Boltzmann physics in the limiting cases and provides a valid solution in the whole transition regime.[9] The reason for the capturing multiple scale flow physics in UGKS is due to the use of an explicit time evolution solution of the kinetic equation for the flux evaluation. This evolution solution takes into account the accumulating effect of particle transport and collision and resolves the gas dynamics from one scale to another scale. So, based on the mesh size and time step, the corresponding flow physics in such a scale can be captured in UGKS for the flux evaluation across a cell interface, which determines the flow evolution. The coupling of the particle transport and collision in the determination of a flux function across a cell interface plays the most important role for the capturing of multiple scale flow physics and connects the dynamics from the Boltzmann to the NS ones smoothly. As shown in the last test case in this paper, if no particle collision is taken into account in the interface flux evaluation for modeling time evolution in a scale being much larger than the particle collision time, any asymptotic preserving (AP) scheme for the kinetic equation is invalid in the continuum flow regime when the cell size is much larger than the particle mean free path. Without using the direct modeling methodology, it will be difficult for any numerical PDE approach to properly connect NS and Boltzmann solutions through mathematical manipulation.[5] Beyond the AP property in the design of kinetic solver, where the Euler solution is usually obtained in the continuum regime, the current UGKS has the unified preserving (UP) property and it is able to capture NS solution in the continuum regime with a cell size being much larger than the particle mean free path, such as the boundary layer calculations.[16]

As shown in Secs. III–V, at low Reynolds number cases, the numerical computation for the direct NS solver becomes difficult and requires a very small time step. This indicates that the NS modeling is not appropriate to such a flow condition, where the particle penetration takes effect. For UGKS, a physical time step, which is independent of Reynolds numbers, can be used uniformly in all flow regimes. This is consistent with the above analysis, where the physical propagating speed is independent of the gas density. The aim of this paper is to figure out the dynamics differences quantitatively between the UGKS and NS modeling and point out the importance to adopt direct modeling for computation of multiple scale flow problem.

III. DISTINCT GOVERNING EQUATIONS AND DIRECT MODELING SCHEME

In order to present the ideas of the conventional CFD simulation and the direct modeling approach, we are going to use the linear advection diffusion equation and the kinetic Boltzmann

Bhatnagar-Gross-Krook (BGK) model for flow description in different scales. The extension of the scheme to gas dynamic equations will be presented as well.

A. Hydrodynamic equation and its connection to kinetic model equation

The kinetic Boltzmann equation and the hydrodynamic Navier-Stokes equations are obtained based on different scale modeling. In the kinetic mean free path scale, the BGK equation models the flow physics as[2]

$$\partial_t f + c\partial_x f = \frac{1}{\tau}(g - f), \tag{1}$$

for the evolution of a gas distribution function f with free transport (left) and collision term (right) effects. In Eq. (1), $f(c, x, t)$ is the velocity distribution function, c is the microscopic particle velocity, g is the equilibrium state, and τ is the collision time. In the hydrodynamic scale with the fluid element approximation, the linear advection-diffusion equation is

$$u_t + au_x = \nu u_{xx}, \tag{2}$$

for the propagation of macroscopic variable u with macroscopic velocity a, and diffusive mechanism with a constant viscosity coefficient ν.

The macroscopic and microscopic quantities are related through

$$u(x, t) = \int_R f(c, x, t)dc. \tag{3}$$

The equilibrium Maxwellian distribution g is

$$g = u\frac{1}{\sqrt{\theta\pi}}\mathrm{e}^{-\frac{(c-a)^2}{\theta}}. \tag{4}$$

θ corresponds to the temperature, which is related to the spread of particle random velocity.

Integrating the particle velocity on both sides of Eq. (1) gives the macroscopic equation

$$\partial_t u + \partial_x F = 0,$$

with the flux

$$F(x, t) = \int_R cf(c, x, t)dc.$$

In the continuum regime, with the underlying physical assumption that the variation of f in the hydrodynamic scale is smooth enough due to substantial particle collisions, the Chapman-Enskog method gives a solution to the dimensionless BGK equation,

$$\tilde{f}^{(N)}(\tilde{c}, \tilde{x}, \tilde{t}) = \sum_{n=0}^{N} \tilde{\tau}^n \tilde{f}_n(\tilde{c}, \tilde{x}, \tilde{t}), \tag{5}$$

where the dimensionless relaxation time approximates the Knudsen number

$$\tilde{\tau} = \frac{\tau U_\infty}{L_\infty} \sim \mathrm{Kn}. \tag{6}$$

In the following, we omit the tilde for simplicity. The first order expansion becomes

$$f^{(1)}(c, x, t) = (u - \tau(c - a)\partial_x u)\frac{1}{\sqrt{\theta\pi}}\mathrm{e}^{-\frac{(c-a)^2}{\theta}}. \tag{7}$$

The corresponding macroscopic flux reads

$$F^{(1)} = au - \frac{\theta\tau}{2}\partial_x u, \tag{8}$$

which leads to the advection-diffusion

$$u_t + au_x = \frac{\theta\tau}{2}u_{xx}.$$

By comparing the coefficient with Equation (2), we have the relation

$$\nu = \frac{\theta\tau}{2}.$$

The expansion (7) converges when τ is small, and Eq. (2) may not be consistent with Eq. (1) when τ gets large.

B. The UGKS and the hydrodynamic equation solver

We consider a discretization of the space-time $\Omega \times [0, T]$ with constant spatial cell size Δx and time step Δt. The basic numerical method is an explicit finite volume method. The evolution equation for the macroscopic conservative variable is

$$U_i^{n+1} = U_i^n + \frac{\Delta t}{\Delta x}(F^n_{i-\frac{1}{2}} - F^n_{i+\frac{1}{2}}), \tag{9}$$

where $F^n_{i+\frac{1}{2}}$ is the time averaged numerical flux at cell interface, which can be obtained from the gas distribution there,

$$F^n_{i+\frac{1}{2}} = \frac{1}{\Delta t}\int_0^{\Delta t}\int_{-\infty}^{\infty} cf(c, x_{i+\frac{1}{2}}, t)dcdt. \tag{10}$$

The above Eq. (9) is a physical balance law in a discretized space. The physics to be captured depends on the modeling of the cell interface distribution function in Eq. (10). As analyzed before, in the hydrodynamic scale, the fluid element representation can be used to model the flux, such as the solver based on Eq. (2). In the kinetic scale, the particle transport and collision will take effect, and the solution from Eq. (1) can be used. In UGKS, the physics to be simulated will depend on the scales of Δx and Δt in Eq. (9) with respect to the particle mean free path and collision time.

For the hydrodynamic solver, we only need to update the above macroscopic conservative flow variable. However, as the gas density reduces, in the transition flow regime the macroscopic flow variable update alone is not enough for the capturing of the peculiarity of the non-equilibrium property, where more degrees of freedom are needed to follow the flow evolution. The UGKS is based on the evolution of both macroscopic variable Eq. (9) and the gas distribution function. The evolution equation for the microscopic velocity distribution function is

$$f_i^{n+1} = \left(1 + \frac{\Delta t}{2\tau}\right)^{-1}\left[f_i^n + \frac{\Delta t}{\Delta x}(\tilde{f}_{i-\frac{1}{2}} - \tilde{f}_{i+\frac{1}{2}}) + \frac{\Delta t}{2}\left(\frac{g^{n+1}}{\tau} + \frac{g^n - f^n}{\tau}\right)\right], \tag{11}$$

where $\tilde{f}_{i+\frac{1}{2}}$ is the time averaged numerical flux for distribution function,[17] which is calculated by

$$\tilde{f}_{i+\frac{1}{2}} = \frac{1}{\Delta t}\int_0^{\Delta t} cf(c, x_{i+\frac{1}{2}}, t)dt. \tag{12}$$

Here we will obtain the time evolution solution of the kinetic BGK Eq. (1) to model the interface fluxes in Eqs. (9) and (11).

For solving the full Boltzmann equation, similar technique can be applied.[9]

For the macroscopic equation solver, Eq. (9) alone is used for the update of macroscopic flow variable. For direct modeling method, the UGKS uses both Eqs. (9) and (11) for the update of flow variable and the gas distribution function. The flux function for both Equations (9) and (11) is based on the same integral solution of Eq. (1) at a cell interface,

$$f(c,x,t) = \frac{1}{\tau}\int_0^t g(c,x-c(t-s),s)\mathrm{e}^{-\frac{t-s}{\tau}}ds + \mathrm{e}^{-\frac{t}{\tau}}f_0(c,x-ct,0), \tag{13}$$

where f_0 is the initial condition. This is a multiple scale transport solution, which covers from the free molecular flow to the hydrodynamic solution. The physics to be presented depends on the ratio of time step $t = \Delta t$ over the particle collision time τ. But, the different choices of the initial condition f_0 at the beginning of each time step determine the different evolution mechanism, i.e., the macroscopic equation solver, or a multiple scale evolution model.

For the linear advection-diffusion Eq. (2), the corresponding scheme used for its solution is the gas-kinetic scheme (GKS) for the update of macroscopic flow variable alone,[14] which is basically a NS solver in the continuum flow regime. Here, the initial condition f_0 in Eq. (13) is constructed based on the Chapman-Enskog expansion, such as Eq. (7). This assumption automatically projects the distribution function to the fluid element modeling, where a small deviation from the equilibriums state is used for the capturing of diffusive effect. For the direct modeling UGKS, the initial condition f_0 is known through the update of the gas distribution function in Eq. (11). Therefore, the departure from the equilibrium depends on the scale, such as the ratio of $\Delta t/\tau$. Note that the cell size and time step are the modeling scales of UGKS.

The GKS is a direct macroscopic Eq. (2) solver through the update of Eq. (9) alone. The interface flux is based on the solution of Eq. (13) with the adoption of the Chapman-Enskog expansion for the initial condition f_0. The use of the Chapman-Enskog expansion makes GKS solve the advection-diffusion equation only. For the UGKS, there is no such an assumption about the form of the initial gas distribution function, and the real scale-dependent distribution function is followed through its evolution. The capability of capturing multiscale physics from UGKS is mainly due to the scale dependent evolution solution of Eq. (13) for the cell interface flux evaluation, which depends on the ratio of the time step $t = \Delta t$ over the particle collision time τ. The capturing of different physics can be easily understood from the solution of Eq. (13). In the kinetic regime, i.e., $\Delta t \le \tau$, the particle free transport from f_0 in Eq. (13) contributes mainly for the flux function. This is identical to modeling of transport part in DSMC and direct Boltzmann solver, the same as many AP schemes using free particle transport for the flux function, such as AP-KFVS. For the scale with $\Delta t \ge \tau$, the collision will gradually take effect. In the hydrodynamic limit, i.e., $\Delta t \gg \tau$, the NS gas distribution from the equilibrium state integration in Eq. (13) will play a dominant role. Therefore, the solution provided in Eq. (13) depends on the ratio $\Delta t/\tau$ or $\Delta x/l$. In the case of the cell size $\Delta x \gg l$ and time step $\Delta t \gg \tau$, the multiple particle collision effect is included in the integral solution Eq. (13), which is beyond the binary collision model in the full Boltzmann collision term. In the transition regime with a cell resolution of multiple mean free path, the solution in Eq. (13) includes the effect of multiple collisions for individual particle. In terms of the flow modeling, based on Eqs. (9) and (11), the UGKS gives a direct modeling equation in all scales, which is beyond the mean free path scale used in the derivation of the Boltzmann equation. Even though the GKS has the same evolution mechanism from the particle free transport to the hydrodynamic evolution in its flux evaluation, the use of the Chapman-Enskog expansion for f_0, or a fixed form of the initial gas distribution function, confines its applicable regime to the near equilibrium regime only in the macroscopic scale. With the use of a dynamically updated gas distribution function as the initial state f_0, the UGKS can give a valid solution in all regimes and use a time step with a fixed Courant-Friedrichs-Lewy (CFL) number, which is independent of the Reynolds number. However, for the GKS, same as other explicit NS solver, its solution is

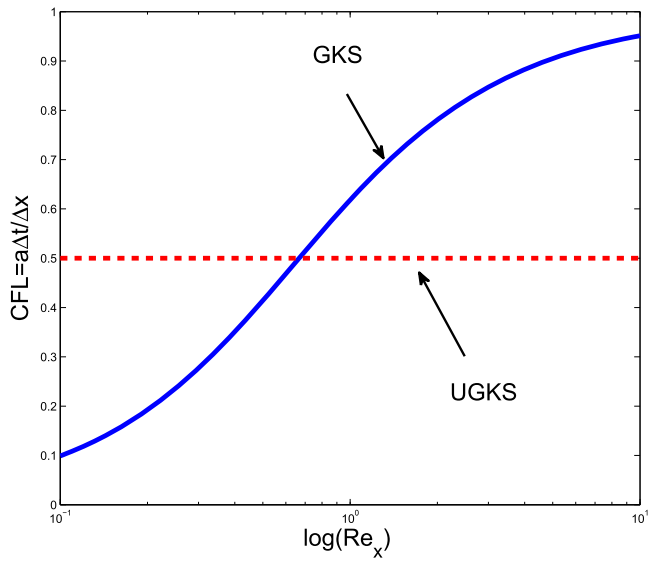

FIG. 3. Maximum CFL number for GKS (NS) and UGKS with different Reynolds numbers.

TABLE I. First set of parameters for the advection-diffusion problem.

	Figs. 4(a) and 4(b)	Figs. 4(c) and 4(d)	Figs. 4(e) and 4(f)	Figs. 4(g) and 4(h)
a	3.0	3.0	3.0	3.0
θ	1.0	1.0	1.0	1.0
τ	1.2	0.24	0.12	0.04
Δx	0.04	0.04	0.04	0.04
Re_x	0.1	0.5	1.0	3.0
$Ma(a/\sqrt{\theta})$	3.0	3.0	3.0	3.0
N	2	2	2	2
a_1	$8/\pi$	$8/\pi$	$8/\pi$	$8/\pi$
a_2	$16/3\pi$	$16/3\pi$	$16/3\pi$	$16/3\pi$
b_1	$\pi/2$	$\pi/2$	$\pi/2$	$\pi/2$
b_2	$3\pi/2$	$3\pi/2$	$3\pi/2$	$3\pi/2$

limited to the continuum flow regime and the time step is severely constrained at the low Reynolds number limit.

Other popular schemes targeting to all flow regimes are the so-called asymptotic preserving (AP) methods, which are mainly based on the direct discretization of the kinetic equation. In this kind of modeling, most schemes adopt the kinetic upwind approach for the construction of the interface flux function, such as the use of the initial condition $f_0(c, x - ct, 0)$ in Eq. (13) only for the flux evaluation at a cell interface even though f_0 itself is a numerically updated one. This approach separates the particle free transport at a cell interface for the flux evaluation from the particle collision inside each cell.

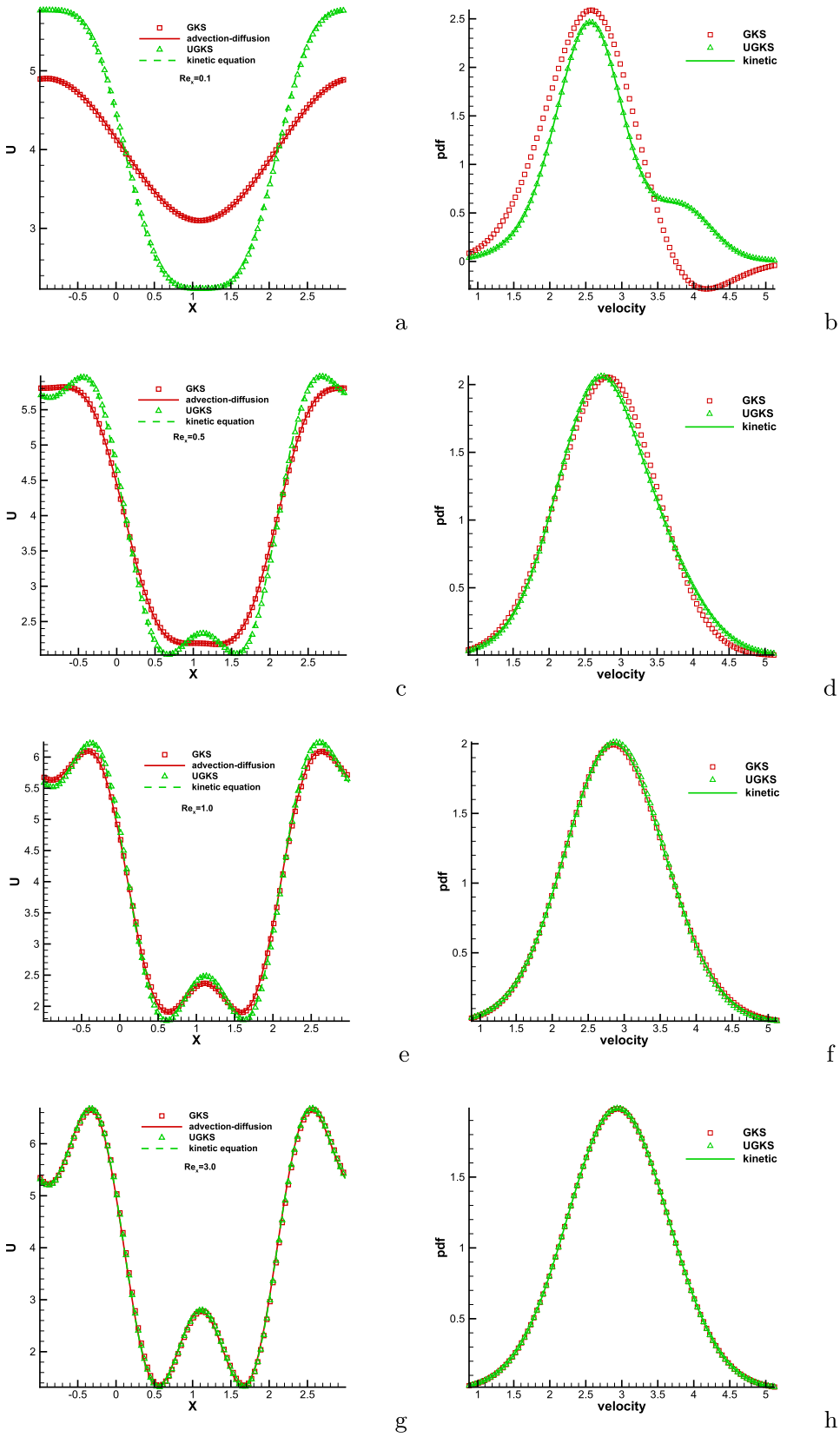

FIG. 4. Left column shows the comparison of the macroscopic quantity u, symbols are the numerical solutions, and lines are the exact solutions of the advection-diffusion equation and the kinetic solutions under a very fine mesh. Right column shows the comparison of the velocity distribution function at $x = 2$, lines are the solutions of kinetic equation under a very fine mesh. From top to bottom, the corresponding cell Reynolds numbers are $Re_x = a\Delta x/(\theta\tau) = 0.1, 0.5, 1.0,$ and 3.0.

TABLE II. Second set of parameters for the advection-diffusion problem.

	Fig. 5(a)	Fig. 5(b)	Fig. 5(c)	Fig. 5(d)	Fig. 5(e)	Fig. 5(f)
a	3.0	3.0	3.0	3.0	3.0	3.0
θ	60	6	60	6	60	6
τ	1.0×10^{-3}	1.0×10^{-3}	1.0×10^{-3}	1.0×10^{-3}	1.0×10^{-3}	1.0×10^{-3}
Δx	0.02	0.02	0.02	0.02	0.02	0.02
Re_x	0.1	10	0.1	10	0.1	10
Ma	0.39	1.22	0.39	1.22	0.39	1.22
N	1	1	1	1	1	1
a	$\exp(0.1\nu\pi^2/4)$	$\exp(0.1\nu\pi^2/4)$	$\exp(2.5\nu\pi^2/4)$	$\exp(2.5\nu\pi^2/4)$	$\exp(10\nu\pi^2/4)$	$\exp(10\nu\pi^2/4)$
b	$\pi/2$	$\pi/2$	$5\pi/2$	$5\pi/2$	$10\pi/2$	$10\pi/2$

It has the same dynamical mechanism as DSMC, even though the initial gas distribution at the beginning of each time step can be modified on purpose. In this approach, the particle free transport will introduce a numerical dissipation which is proportional to the mesh size. This is also the reason why the DSMC needs a mesh size smaller than the particle mean free path. In the continuum regime, in order to reduce the numerical dissipation, such as in the calculation of high Reynolds

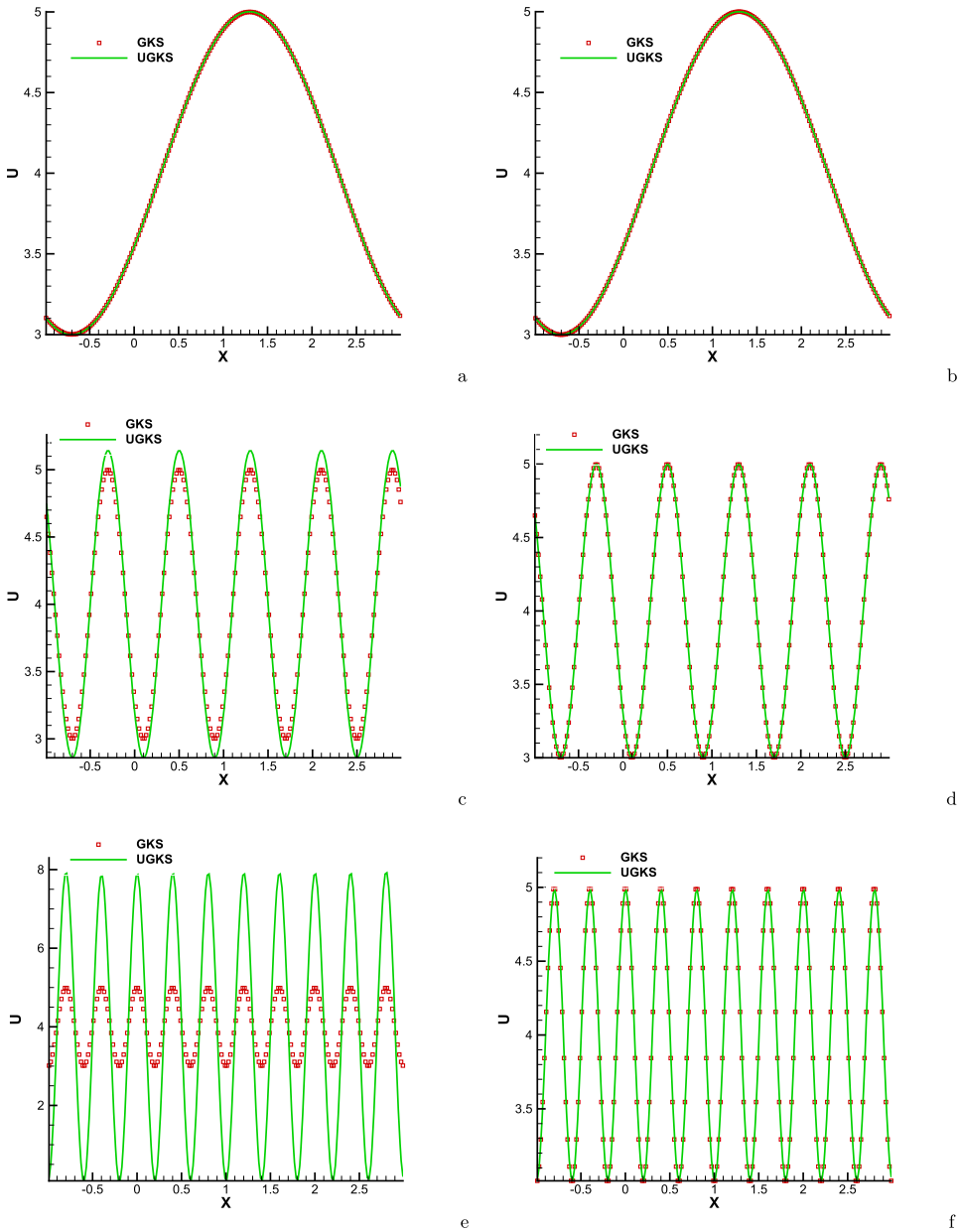

FIG. 5. In current calculation, $Re_x = \frac{a\Delta x}{\theta\tau}$ with $a = 3, \Delta x = 0.02$, and $\tau = 1.0 \times 10^{-3}$. Here θ takes different values to give different Re_x, and the particle mean free path is $\ell \sim \sqrt{\theta}\tau$. Even with the same Re_x, the local Knudsen numbers (mean free path over wavelength) are different. The parameters for the first row ((a) and (b)) are $N = 1$, $a_1 = \exp(0.1\nu\pi^2/4)$, $b_1 = \pi/2$. The parameters for the second row ((c) and (d)) are $N = 1$, $a_1 = \exp(2.5\nu\pi^2/4)$, $b_1 = 5\pi/2$. The parameters for the third row ((e) and (f)) are $N = 1$, $a_1 = \exp(10\nu\pi^2/4)$, $b_1 = 10\pi/2$. The corresponding Re_x and local Knudsen number $Kn_c = \ell/\text{wavelength}$, such as (Re_x, Kn_c), are: $(0.1, 0.01)$ (a), $(0.1, 0.05)$ (c), $(0.1, 0.1)$ (e), $(10, 0.001)$ (b), $(10, 0.005)$ (d), and $(10, 0.01)$ (f).

TABLE III. Parameters for the shear layer problem.

	Fig. 8	Fig. 9	Fig. 10	Fig. 11	Fig. 12	Fig. 13
Kn	5.0×10^{-3}	5.0×10^{-3}	5.0×10^{-3}	5.0×10^{-3}	5.0×10^{-3}	5.0×10^{-3}
$\mu(T=400\,\mathrm{K})$	3.996×10^{-3}	3.996×10^{-3}	3.996×10^{-3}	3.996×10^{-3}	3.996×10^{-3}	3.996×10^{-3}
τ_{ph}	5.12×10^{-3}	5.12×10^{-3}	5.12×10^{-3}	5.12×10^{-3}	5.12×10^{-3}	5.12×10^{-3}
Output time	5.12×10^{-3}	5.12×10^{-2}	5.12×10^{-1}	4	40	400
dx/ℓ (GKS)	0.1	0.4	2.0	10.0	10.0	33.33
dt/τ_{ph} (GKS)	1.96×10^{-3}	1.56×10^{-2}	3.91×10^{-1}	7.81	7.81	26.06
dx/ℓ (UGKS)	0.1	0.4	2.0	10.0	50.0	250
dt/τ_{ph} (UGKS)	1.65×10^{-2}	6.61×10^{-2}	3.78×10^{-1}	1.89	8.25	41.25

number boundary layer, this kind of AP approach still needs to use a mesh size smaller than the particle mean free path for the capturing of accurate viscous solution. Practically, under such a constraint, this kind of methods can be hardly used in engineering applications for the multiple scale flow problems. The scheme AP-KFVS presented in Sec. IV is basically such a scheme, which is the same as UGKS except the flux evaluation.

IV. DYNAMICAL DIFFERENCES IN CASE STUDIES

A. Linear advection-diffusion process and the corresponding multiple scale solution

To identify the dynamical differences quantitatively from different modeling, we first solve Eq. (2) for the advection diffusion solution in the domain $x \in [-1, 3]$ with the periodic boundary condition. The initial condition is set as

$$u_0(x) = 4 + \sum_{i=1}^{N} a_i \sin(b_i x). \tag{14}$$

For the linear advection-diffusion equation, the analytic solution is given by

$$u(x,t) = 4 + \sum_{i=1}^{N} a_i e^{-b_i^2 \nu t} \sin(b_i(x-at)). \tag{15}$$

Based on the GKS (advection-diffusion solution) and the UGKS (multiscale modeling solution), in the high Reynolds number limit, both results are identical in the hydrodynamic regime. The current study is mostly on the transition regime at the low Reynolds number limit, where both fluid element and particle penetration play an important role. In the low Reynolds number regime, the stability condition for GKS, like many other advection-diffusion solvers, becomes restricted. The time step is limited by $\Delta t < (\Delta x)^2/(2\nu)$. However, for the UGKS, a necessary stability condition is due to the particle velocity range used to discretize the velocity space. In other words, for the UGKS, the time step is determined by the CFL condition only,

$$\Delta t \le \frac{\Delta x}{|a| + 3\sqrt{\theta}}. \tag{16}$$

The stability condition for GKS and UGKS is shown in Fig. 3 with $a = 3$ and $\theta = 1.0$ under different cells' Reynolds number, i.e., $Re_x = a\Delta x/(\theta\tau)$.

Under the stability condition, the solutions from the above two schemes behave differently with the variation of Reynolds numbers. By setting the parameters $a = 3$, $\theta = 1$, $\Delta x = 0.04$, and $N = 2$ with $a_1 = 8/\pi$, $b_1 = \pi/2$, $a_2 = 16/3\pi$, $b_2 = 3\pi/2$, we compare the solutions of GKS and UGKS with cell Reynolds number $\mathrm{Re}_x = 0.1, 0.5, 1.0, 3.0$. The detail values of parameters are listed in Table I. In Fig. 4, we plot

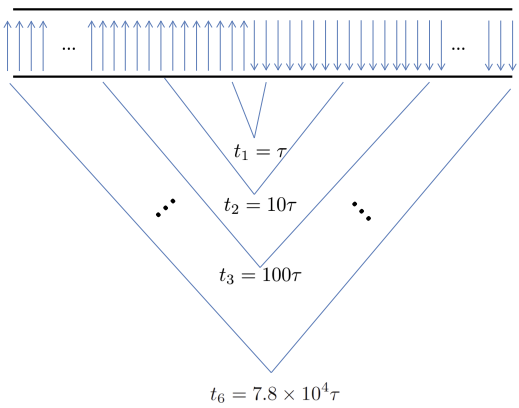

FIG. 6. Multiscale flow evolution for a shear layer, where t_i is the evolution time and τ is the particle collision time. The corresponding computational domain is changing with t_i with different cell sizes Δx relative to the particle mean free path ℓ.

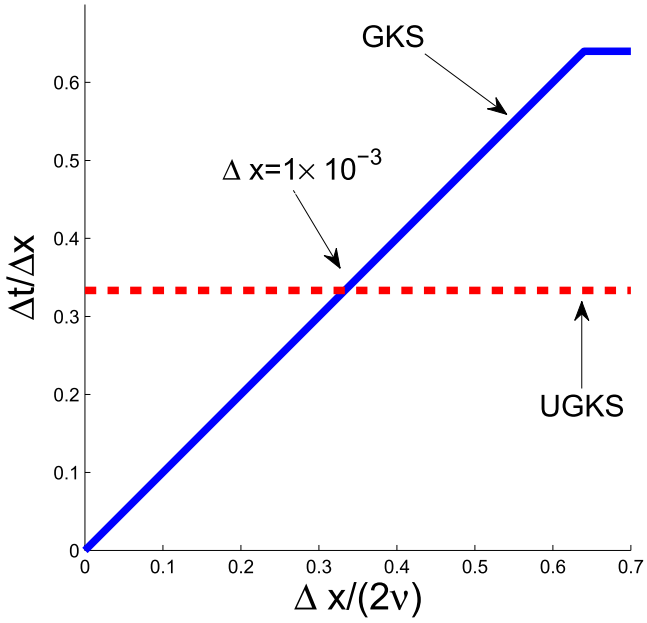

FIG. 7. Time step v.s. cell size.

the macroscopic quantity u and the velocity distributions at $t = 0.7$ and $x = 2$. At high Reynolds number regime, both advection-diffusion equation and UGKS solutions are consistent, and the macroscopic description is a valid model. When Reynolds number decreases to be less than 1, the advection-diffusion solutions deviate from the UGKS solutions. Especially, when $\mathrm{Re}_x = 0.1$, the distribution function corresponding to the advection diffusion model, which is obtained from the Chapman-Enskog expansion, can become negative in certain particle velocity region. The possible negative particle velocity distribution and the severe time step limitation indicate that the advection-diffusion equation is not applicable for capturing flow physics in this regime. For low Reynolds number flow, the time step used in UGKS is independent of Reynolds number, which is consistent with the physical reality.

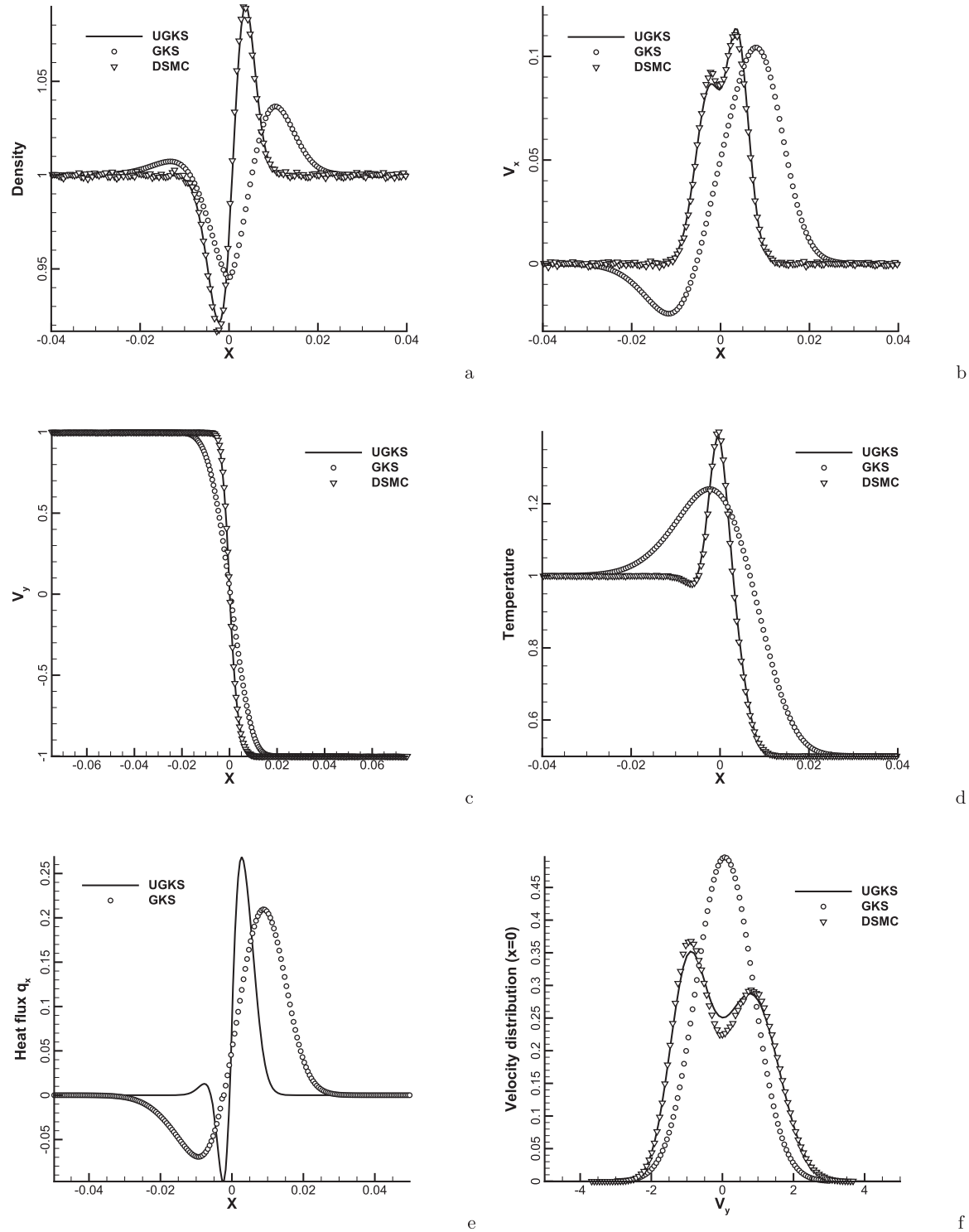

FIG. 8. UGKS, GKS, and DSMC results at $t = 5.12 \times 10^{-3}$ ($t = \tau_{ph}$): (a) density; (b) x-velocity; (c) y-velocity; (d) temperature; (e) x direction heat flux; (f) velocity distribution at $x = 0$. For GKS $dx/\ell = 0.1$, $dt = 1.96 \times 10^{-3}\tau_{ph}$, and for UGKS $dx/\ell = 0.1$, $dt = 1.65 \times 10^{-2}\tau_{ph}$, and $\mu = 2.117 \times 10^{-5}$Ns m^{-2} at $t = 273$ K.

Next, we fix $\tau = 1.0 \times 10^{-3}$ and compare the GKS and UGKS solutions at different Reynolds numbers by changing the dimensionless temperature θ. The values of parameters are listed in Table II. The results are shown in Fig. 5 with Reynolds numbers $Re_x = (0.1, 10)$, and different wave frequencies. It can be observed that when the Reynolds number is relatively large, the GKS solution agrees with the UGKS one and the advection-diffusion equation is a valid model. At high temperature, the mean free path gets large, i.e., $\ell \sim \tau\sqrt{\theta}$. Therefore, the local Knudsen number, which is defined as the ratio of particle mean free path over the local characteristic length, such as the wavelength of the physical solution, becomes large. In the low Reynolds number limit, with the increment of the local Knudsen number, the advection-diffusion solution deviates from the kinetic solution. Even with the same Re_x, different wavelength flow structures have

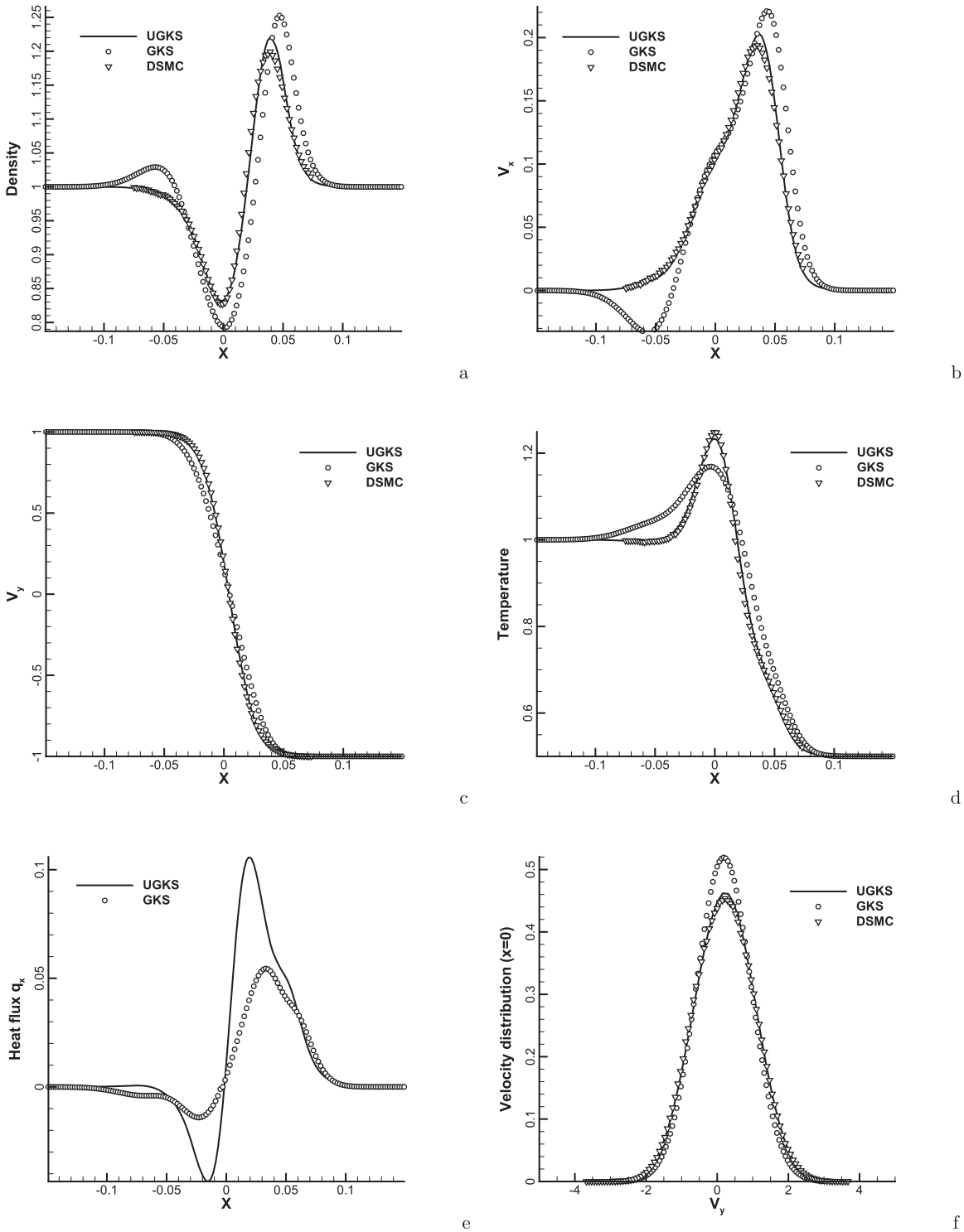

FIG. 9. UGKS, GKS, and DSMC results at $t = 5.12 \times 10^{-2}$ ($t = 10\tau_{ph}$): (a) density; (b) x-velocity; (c) y-velocity; (d) temperature; (e) x direction heat flux; (f) velocity distribution at $x = 0$. For GKS $dx/\ell = 0.4$, $dt = 1.56 \times 10^{-2}\tau_{ph}$, and for UGKS $dx/\ell = 0.4$, $dt = 6.61 \times 10^{-2}\tau_{ph}$, and $\mu = 2.117 \times 10^{-5}$Ns m^{-2} at $t = 273$ K.

different local Knudsen numbers and correspond to different time evolutions. For a real flow problem, it will be hard to set up a condition for the validity of the advection diffusion equation if the flow is composed of all kinds of wave structures with different spatial frequencies. For a real flow problem, such as the turbulent boundary layer, the flow velocity contains high frequency modes in both space and time.[11,18] Therefore, the local Knudsen number depends on the flow structure and it should be careful to use a single hydrodynamic equation to describe all frequency mode evolutions.

B. The NS solution and the multiscale modeling solution

We present the simulation results of a shear layer using different modeling schemes.

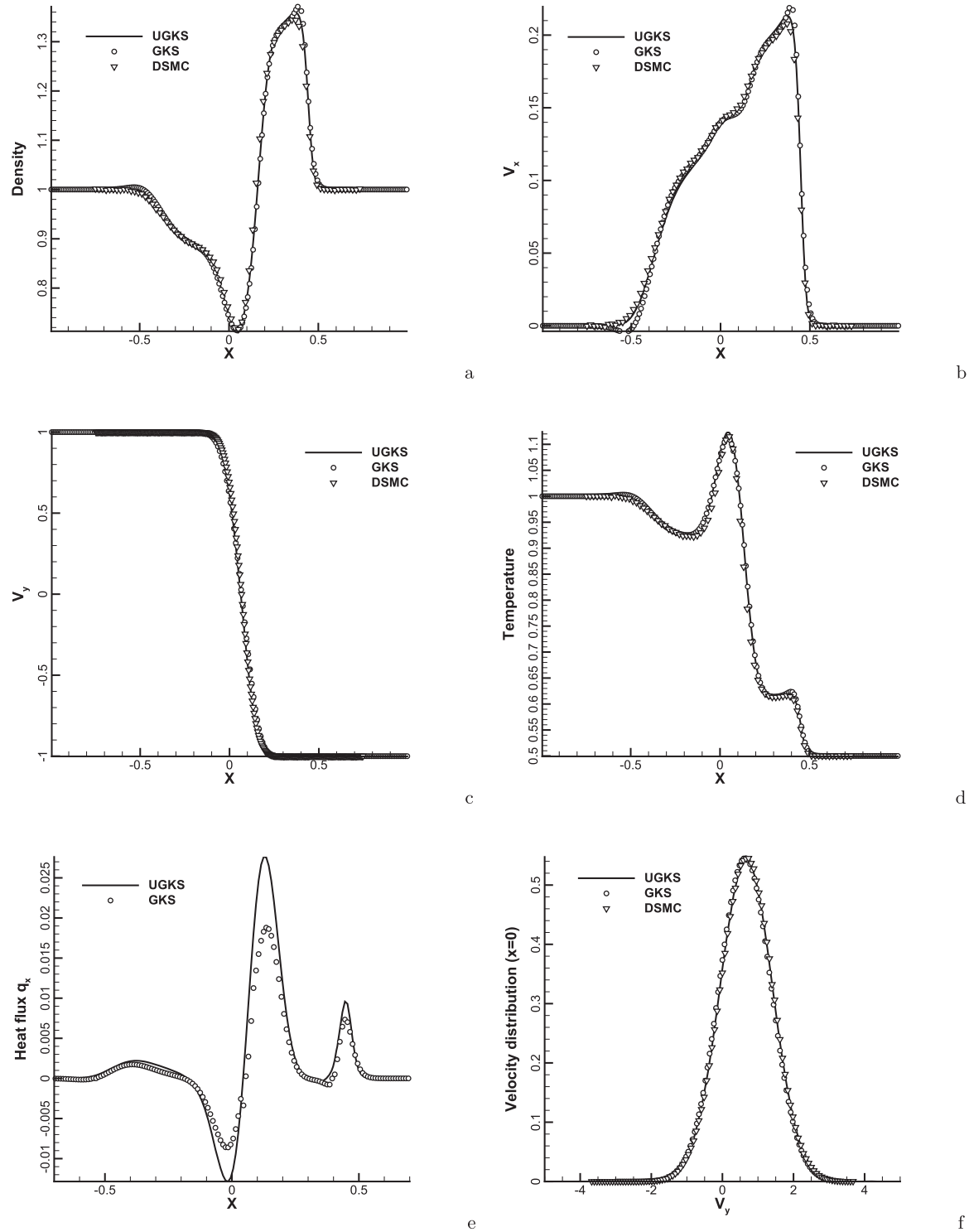

FIG. 10. UGKS, GKS, and DSMC results at $t = 5.12 \times 10^{-1}$ ($t = 100\tau_{ph}$): (a) density; (b) x-velocity; (c) y-velocity; (d) temperature; (e) x direction heat flux; (f) velocity distribution at $x = 0$. For GKS $dx/\ell = 2$, $dt = 3.91 \times 10^{-1}\tau_{ph}$, and for UGKS $dx/\ell = 2$, $dt = 3.78 \times 10^{-1}\tau_{ph}$, and $\mu = 2.117 \times 10^{-5}$Ns m^{-2} at $t = 273$ K.

The GKS gives the Navier-Stokes solution and the UGKS captures a multiscale physical solution. The VHS model of argon gas is used in the simulation. The viscosity coefficient depends on the temperature with a power index $\omega = 0.811$, and relative molecular mass $M = 39.984$. The initial condition is given as

$$(n, U, V, T) = \begin{cases} (1.332\,91 \times 10^{25}/\mathrm{m}^3, 0, \ \ 408.05\ \mathrm{m/s}, 400\ \mathrm{K}), & x \le 0, \\ (1.332\,91 \times 10^{25}/\mathrm{m}^3, 0, -408.05\ \mathrm{m/s}, 200\ \mathrm{K}), & x > 0. \end{cases} \tag{17}$$

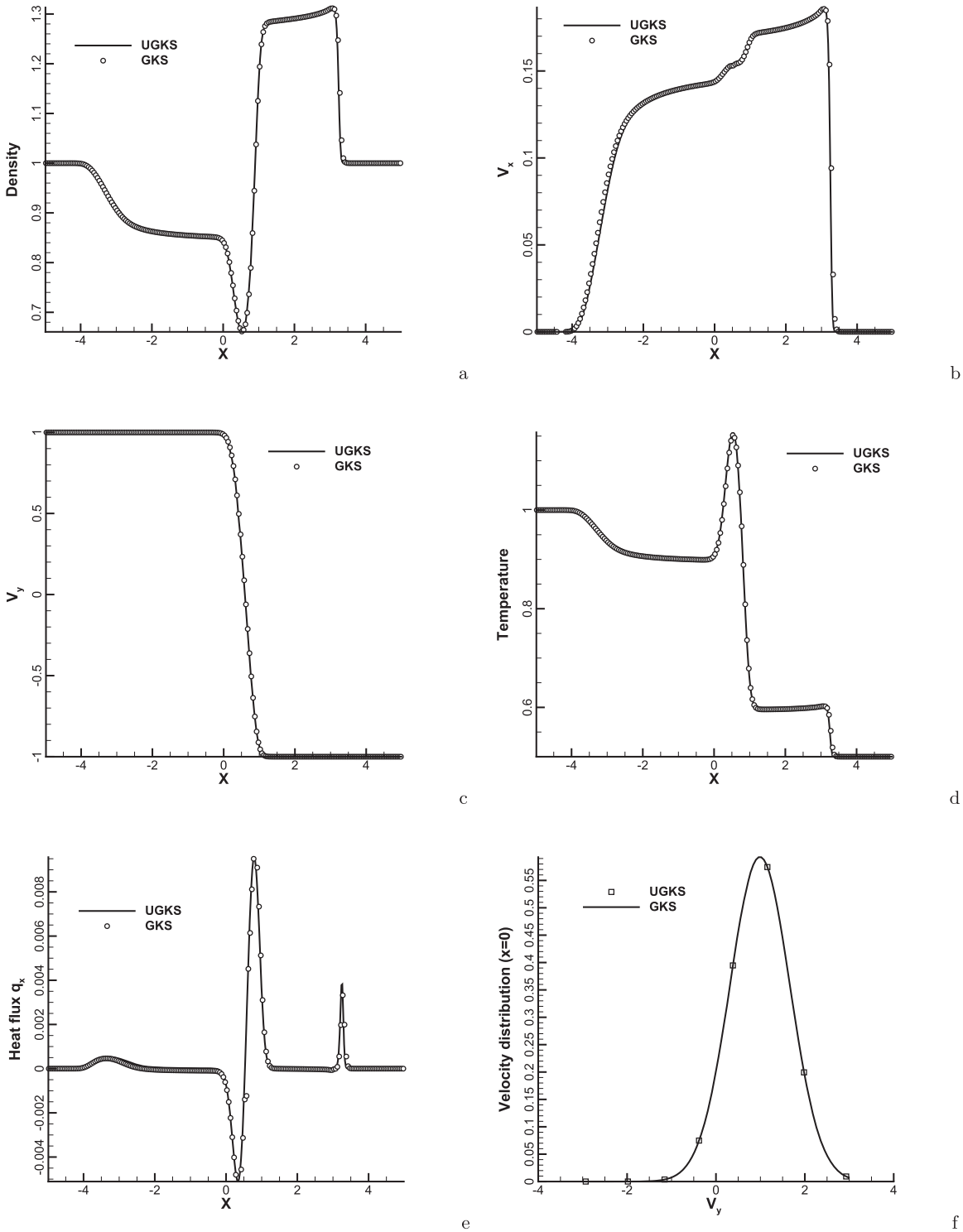

FIG. 11. UGKS, GKS, and DSMC results at $t = 4$ ($t = 781.76\tau_{ph}$): (a) density; (b) x-velocity; (c) y-velocity; (d) temperature; (e) x direction heat flux; (f) velocity distribution at $x = 0$. For GKS $dx/\ell = 10$, $dt = 7.81\tau_{ph}$, and for UGKS $dx/\ell = 10$, $dt = 1.89\tau_{ph}$.

The Knudsen number $Kn = \ell/L_\infty$ is fixed to be 5.0×10^{-3} at the temperature of 300 K, with mean free path $\ell = 0.1$ μm and mean collision time as $\tau_{ph} = 0.250\,786\,4$ ns. The reference viscosity of argon is $\mu = 2.117 \times 10^{-5}$ Pa s at t = 273 K. The integral solution of the Shakhov model is used in the flux evaluation of the UGKS to give a consistent Prandtl number Pr = 2/3.[15] For GKS and UGKS calculations, non-dimensional variables are used according to the reference variables $\rho_\infty = 0.883\,719\,33$ kg/m^3, $L_\infty = 20$ μm, U_∞ = 408.05 m/s, and T_∞ = 400 K. The values of parameters are listed in Table III.

Since we are going to study a time-dependent multiple scale problem, the solutions to be obtained depend on the output time, see Fig. 6, where the computational domain with a fixed number of grid points changes with the domain of influence from the initial singular point. Therefore, the mesh

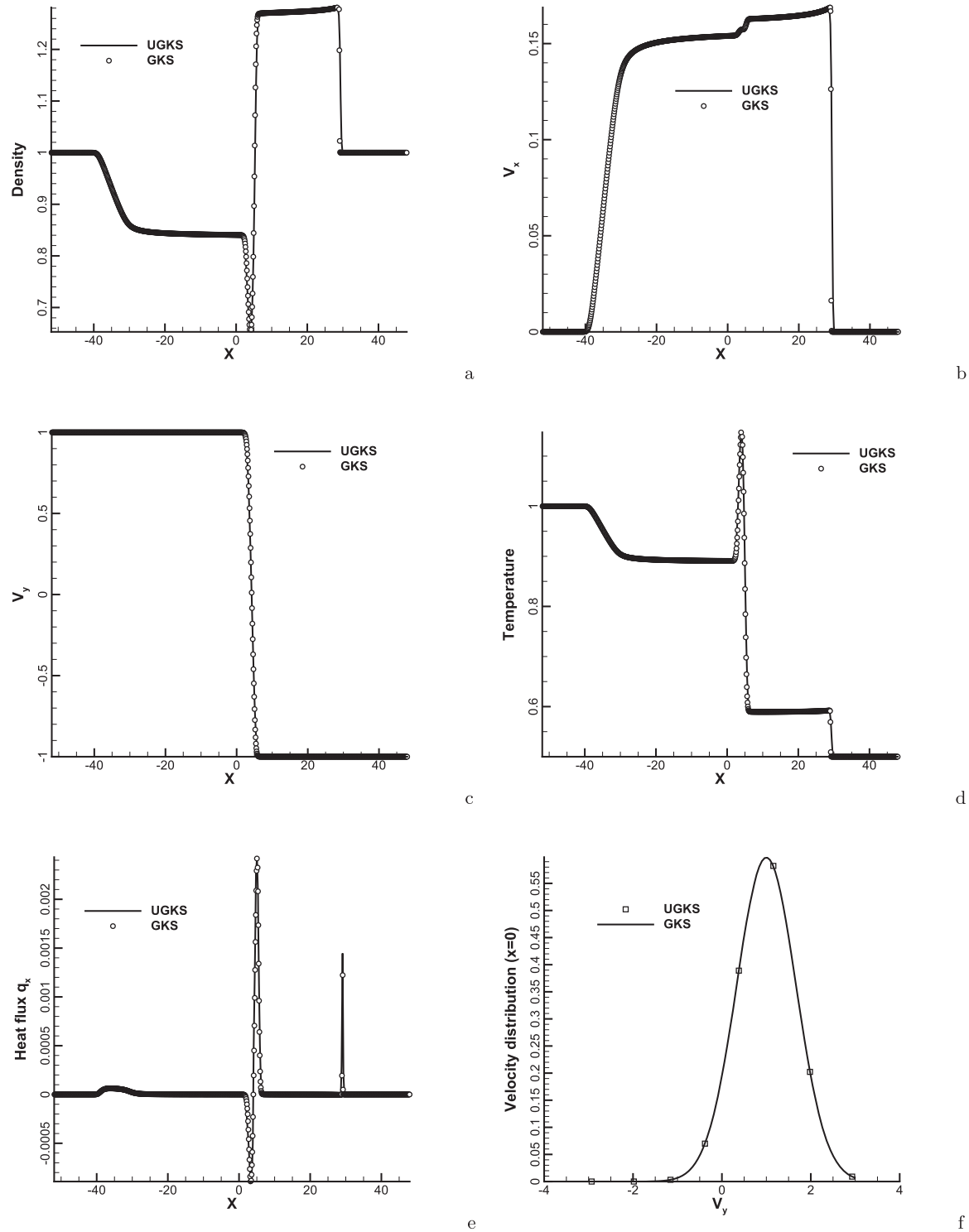

FIG. 12. UGKS, GKS results at t = 40 (t = 7817.64τ_{ph}): (a) density; (b) x-velocity; (c) y-velocity; (d) temperature; (e) x direction heat flux; (f) velocity distribution at x = 0. For GKS dx/ℓ = 10, dt = 7.81τ_{ph} (1000 symbols plotted), and for UGKS dx/ℓ = 50, dt = 8.25τ_{ph}.

sizes are set to different values initially for different output times. Same as the last case, the time steps used for the GKS and UGKS are shown in Fig. 7, where the GKS or NS modeling has severe time step limitation at low Reynolds number limit, but the UGKS uses a uniform CFL number, even though the UGKS can use a large time step as well with stability consideration only.

We plot the density, velocity, temperature, heat flux, as well as the velocity distribution functions at times $t_1 = 5.12 \times 10^{-3}$, $t_2 = 5.12 \times 10^{-2}$, $t_3 = 5.12 \times 10^{-1}$, $t_4 = 4$, $t_5 = 40$, and $t_6 = 400$ with a changeable cell size in order to identify the shear solution in different scales. For GKS, the cell number in x-direction is 150 for Fig. 9, 200 for Figs. 8, 10, and 11, 800 for Fig. 12, and 6000 for Fig. 13. For UGKS, the cell number in x-direction is 150 for Fig. 9, 200 for Figs. 8, 10, and 11, 400 for Fig. 12, and 800 for Fig. 13. The computation confirms that the time step for GKS is limited to be small when the cell Reynolds number is small, as shown in Fig. 7.

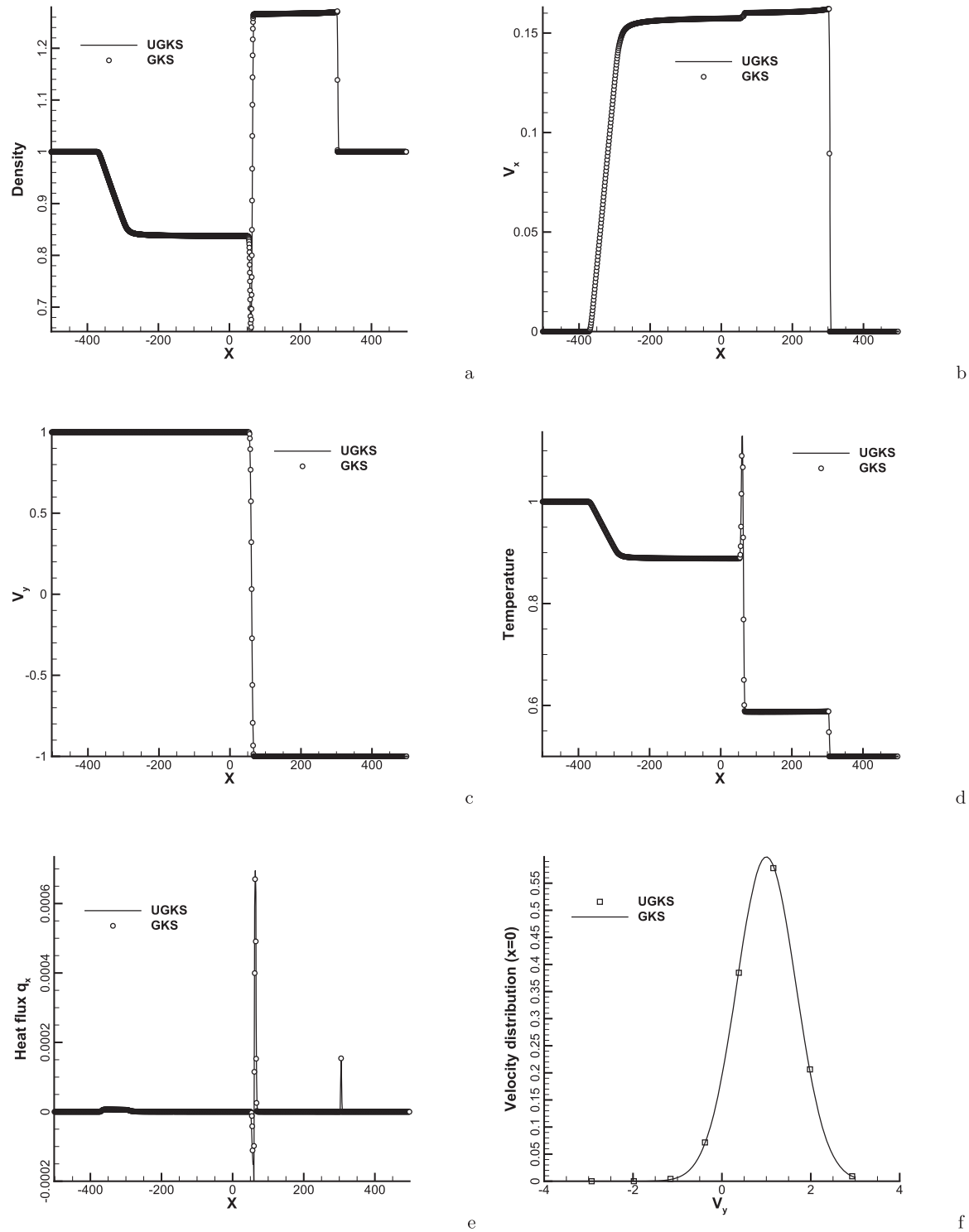

FIG. 13. UGKS and GKS results at $t = 400$ ($t = 78\,176.40\tau_{ph}$): (a) density; (b) x-velocity; (c) y-velocity; (d) temperature; (e) x direction heat flux; (f) velocity distribution at $x = 0$. For GKS $dx/\ell = 33.33$, $dt = 26.06\tau_{ph}$ (1000 symbols plotted), and for UGKS $dx/\ell = 250$, $dt = 41.25\tau_{ph}$.

As a reference, the DSMC solution is also provided in the rarefied regime up to time $t = 100\tau$. For time $t > 100\tau$, due to its computational cost, the DSMC solution is not provided. Since it is relatively difficult for DSMC to get the heat flux from the total energy transport, the heat flux from DSMC is absent. By comparing UGKS solution with the DSMC solution in Figs. 8–10 and GKS solution in Figs. 8–13, it is clear that UGKS is valid in all regimes from the kinetic $t \simeq \tau$ to the hydrodynamic one $t \gg \tau$. Both GKS and UGKS solutions converge in the hydrodynamic regime. To get solutions at all times $t \leq 5.12 \times 10^{-1}$, the UGKS uses 10 000 velocity points. For $t_1 = 5.12 \times 10^{-3}$, the computational time for UGKS is 183 s on a 3.40 GHz 4-core CPU, which is approximately 1% of the computational time of the DSMC. For the case $t > 4$, as the velocity distribution is close to Maxwellian, 64 Gauss quadrature points are used in velocity space. To get the solution up to $t = 400$, the UGKS needs only 13 s on a 3.40 GHz 4-core CPU. In order to identify the importance of the flux function in the construction of the unified scheme, we will also present the solution from the AP-KFVS, where the upwind approach is used for the flux evaluation, such as the use of f_0 only in Eq. (13). In Fig. 14, we show the enlarged slip layer region close to $x = 60$ and compare UGKS with the second order AP-KFVS solution.[5] The cell size and time step of AP-KFVS is exactly the same as UGKS. It can be proved that the up-wind flux introduces numerical dissipation proportional to the time step, which is obvious too much when $\Delta t \gg \tau$.[5]

Since a much larger cell size is used for the hydrodynamic solution for the cases of $t \gg \tau$ and $\Delta x \gg \ell$, in this limit the discontinuity is not well-resolved by both GKS and UGKS when a much larger cell size is used in comparison with particle mean free path. A shock capturing approach is basically obtained for both schemes. In order to give a more accurate physical representation, the cell size used in UGKS should depend on the flow physics to be resolved. In the highly dissipative region, a small cell size can be used to capture the non-equilibrium dynamics, and in the smooth region a large cell size for the hydrodynamic solution can be used for its evolution. The UGKS has the capability to give different flow physics in different regions, such that from particle free transport to the hydrodynamic wave propagation. Besides the multiple scale nature of the UGKS, it is found that even in the continuum flow regime the UGKS is much more robust than GKS or NS solver. In most times, the UGKS can use a larger cell size than that used in GKS for capturing an accurate physical solution, such as Fig. 13. It indicates that an appropriate physical modeling will affect the numerical performance. The modeling and computation are

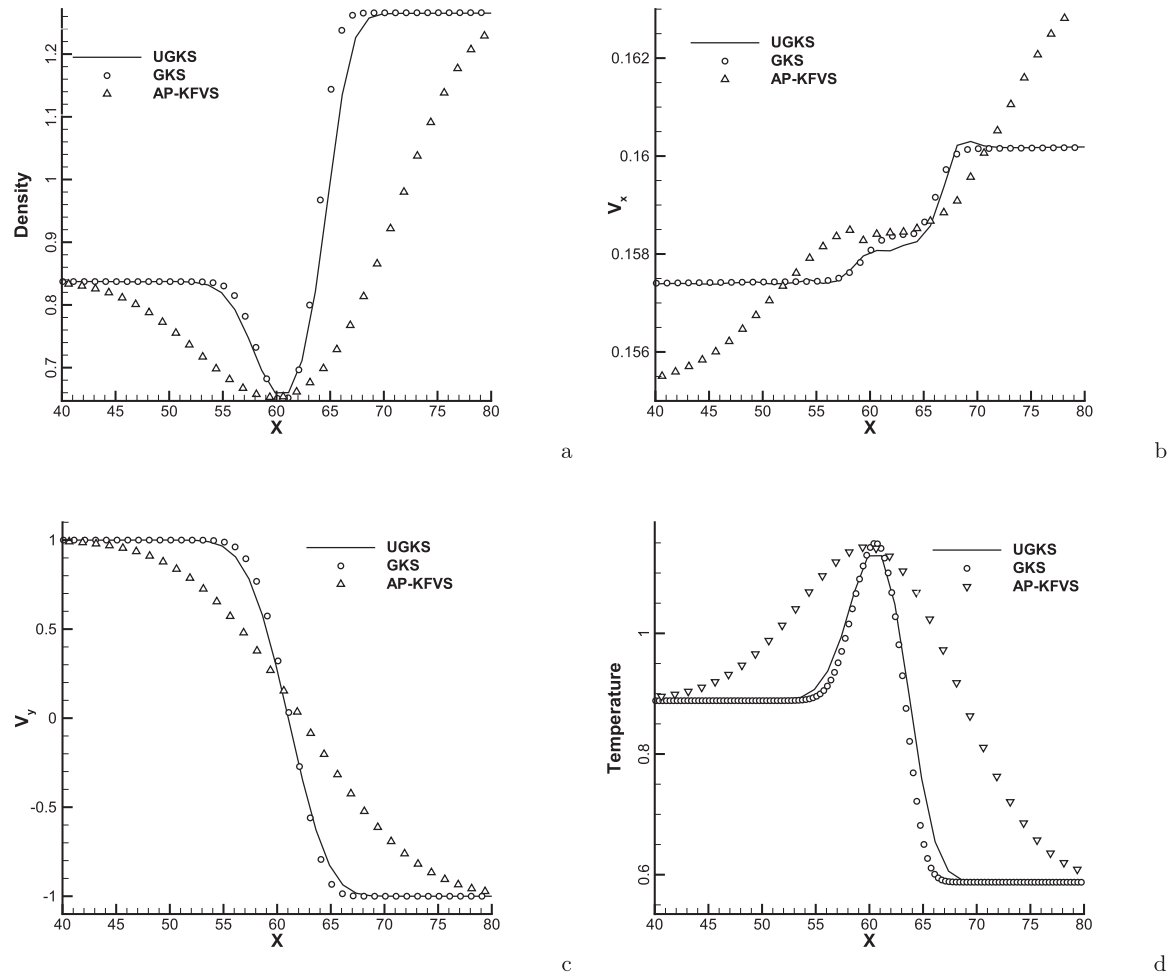

FIG. 14. Local enlarged solutions of UGKS, GKS, AP-KFVS results at $t = 400$ ($t = 78\,176.40\tau_{ph}$): (a) density; (b) x-velocity; (c) y-velocity; (d) temperature. For GKS $dx/\ell = 33.33$, $dt = 26.06\tau_{ph}$ (1000 symbols plotted), for UGKS $dx/\ell = 250$, $dt = 41.25\tau_{ph}$, and for AP-KFVS $dx/\ell = 250$, $dt = 41.25\tau_{ph}$.

inseparable for capturing a valid solution with multiple scale nature.

V. CONCLUSION

The gas dynamics evolution has an intrinsic multiple scale nature, which corresponds to scale-dependent dynamics for different flow structures. Its physical modeling depends on the scale relative to the particle mean free path. In this paper, we present two physical descriptions for gas evolution. One is the macroscopic fluid element approach, i.e., the NS equations and the other is a multiscale modeling algorithm UGKS. This study presents the limitation of the macroscopic level modeling based on the fluid element assumption. In the low Reynolds number limit, the NS approach imposes severe time-step constraint, such as $\Delta t < (\Delta x)^2/\nu$, for the capturing of flow evolution. This time step limitation is purely an artificial one due to inappropriate macroscopic modeling for the emerging microscopic scale physics. In other words, the computational difficulties associated with the NS solution at low Reynolds number case are from its physical inconsistency, due to the use of the fluid element modeling in the region where the particle penetration effect plays an important role. For the direct modeling method, such as the UGKS, due to its capability to have a smooth transition between the fluid element and particle free penetration mechanism with a variation of scales, the time step used in the computation is independent of Reynolds number, which is consistent with the physical propagating speed in different regimes. This study indicates that the multiscale nature of gas dynamics requires new methodology instead of targeting on a specific governing equation. The direct modeling and computation for gas dynamics can provide an indispensable tool for the capturing of physical reality with large scale variations. For a complicated flow structure, the dynamics for different frequency modes may be controlled by different governing equations. The numerical computation is not necessarily to get the exact solution of a specific governing equation but to model the flow physics in a scale to resolve it, and construct the corresponding evolution equation in such a scale. The UGKS provides both equations and the evolution solution. It goes beyond the traditional numerical PDE principle for the computation. The direct modeling methodology provides a new way for scientific computing, especially for the multiple scale transport, such as rarefied flow,[7] radiative transfer,[13] phonon heat transfer,[6] and plasma physics.[10] In the direct modeling scheme, we have no fixed scale and fixed governing equation. All well developed principles in numerical PDE, such as well-posedness, consistency, and convergence, have to be reformulated under the direct modeling methodology for the flow simulation with multiple scale nature.

ACKNOWLEDGMENTS

We would like to thank Professor Q. H. Sun for providing the DSMC solutions and all reviewers for their constructive comments. The current research is supported by Hong Kong research grant council (Grant Nos. 16207715, 16211014, and 620813) and Grant Nos. NSFC-91330203 and 91530319.

[1] V. V. Aristov, *Direct Methods for Solving the Boltzmann Equation and Study of Nonequilibrium Flows* (Kluwer Academic Publishers, 2001).
[2] P. L. Bhatnagar, E. P. Gross, and M. Krook, "A model for collision processes in gases I: Small amplitude processes in charged and neutral one-component systems," Phys. Rev. **94**, 511–525 (1954).
[3] G. A. Bird, *Molecular Gas Dynamics and the Direct Simulation of Gas Flows* (Oxford Science Publications, 1994).
[4] S. Chapman and T. G. Cowling, *The Mathematical Theory of Non-Uniform Gases* (Cambridge University Press, 1990).
[5] S. Z. Chen and K. Xu, "A comparative study of an asymptotic preserving scheme and unified gas-kinetic scheme in continuum flow limit," J. Comput. Phys. **288**, 52–65 (2015).
[6] Z. L. Guo and K. Xu, "Discrete unified gas kinetic scheme for multiscale heat transfer based on the phonon Boltzmann transport equation," Int. J. Heat Mass Transfer **102**, 944–958 (2016).
[7] D. W. Jiang, "Study of the gas-kinetic scheme based on the analytic solution of model equations," Ph.D. thesis, China Aerodynamics Research and Development Center, 2016.
[8] L. D. Landau and E. M. Lifshitz, *Fluid Mechanics* (Pergamon Press, London, 1959).
[9] C. Liu, K. Xu, Q. H. Sun, and Q. D. Cai, "A unified gas-kinetic scheme for continuum and rarefied flow IV: Full Boltzmann and model equations," J. Comput. Phys. **314**, 305–340 (2016).
[10] C. Liu and K. Xu, "A unified gas-kinetic scheme for multiscale plasma transport," preprint arXiv:1609.05291v1 (2016).
[11] H. Schlichting and K. Gersten, *Boundary Layer Theory*, 8th ed. (Springer, 2000).
[12] Y. Sone, "Flows induced by temperature fields in a rarefied gas and their ghost effect on the behavior of a gas in the continuum limit," Annu. Rev. Fluid Mech. **32**, 779C811 (2000).
[13] W. J. Sun, S. Jiang, K. Xu, and S. Li, "An asymptotic preserving unified gas kinetic scheme for frequency-dependent radiative transfer system," J. Comput. Phys. **302**, 222–238 (2015).
[14] K. Xu, "A gas-kinetic BGK scheme for the Navier-Stokes equations and its connection with artificial dissipation and Godunov method," J. Comput. Phys. **171**, 289–335 (2001).
[15] K. Xu, *Direct Modeling for Computational Fluid Dynamics: Construction and Application of Unified Gas-Kinetic Schemes* (World Scientific, Singapore, 2015).
[16] K. Xu, "To overcome memory barrier of kinetic solvers for non-equilibrium flow study," Sci. Bull. **62**, 99–101 (2017).
[17] K. Xu and J. C. Huang, "A unified gas-kinetic scheme for continuum and rarefied flows," J. Comput. Phys. **229**, 7747–7764 (2010).
[18] Y. Zhu, C. Zhang, X. Chen, H. Yuan, J. Wu, S. Chen, C. Lee, and M. Gad-el-Hak, "Transition in hypersonic boundary layers: Role of dilatational waves," AIAA J. **54**, 3039–3049 (2016).